Polish Journal of Medical Physics and Engineering
The Journal of Polish Society of Medical Physics
ISSN 1898-0309, doi: 10.2478/pjmpe-2026-0010

June 2026
Vol 32, Issue 2

Scientific Paper

Comparative Evaluation of ICG Signal Processing Techniques for Detecting Caffeine-Induced Hemodynamic Changes

Ilona Karpiel[1,ABCDEF*], Stefan Gaździński[2,EF], Anna Przewodzka[2,B], Klaudia Duch[3,CD*], Marcin Jonik[1,CD], Mirella Kluza[1,4, CD]

[1]*Łukasiewicz Research Network— Krakow Institute of Technology, Zakopiańska 73, Kraków, 30-418, Poland*
[2]*Department of Neuroimaging, Military Institute of Aviation Medicine, Krasińskiego 54/56, 01-755, Warsaw, Poland*
[3]*Faculty of Science and Technology, Institute of Biomedical Engineering, The University of Silesia in Katowice, 75 Pułku Piechoty 1a, 41-500 Chorzów, Poland*
[4]*Faculty of Biomedical Engineering, Department of Medical Informatics and Artificial Intelligence, Silesian University of Technology, Roosevelta 40, 41-800 Zabrze, Poland*
**Corresponding author: Ilona Karpiel; ilona.karpiel@kit.lukasiewicz.gov.pl; Klaudia Duch; klaudia.duch@us.edu.pl*

(received 20 January 2026; revised 13 April 2026; accepted 04 May 2026)

Abstract

Introduction: The study aims to evaluate the effectiveness of three methods for detecting fiducial points in the impedance cardiography (ICG) signal in the context of subtle hemodynamic changes induced by caffeine intake. The compared approaches include: time-domain detection (CPDA), extrema-based analysis (EBA) and wavelet transform analysis (WTA).

Material and methods: The study involved 20 healthy volunteers, with cardiovascular parameters such as stroke volume (SV), cardiac output (CO) and heart rate (HR) assessed before and after coffee consumption.

Results: Comparative analysis showed that WTA provided the lowest variability of hemodynamic parameters, with standard deviations of ±1.54 for CO and ±21.82 for SV, compared with ±1.76 and ±33.77 for EBA and ±1.92 and ±43.59 for CPDA, respectively. Repeated-measures ANOVA revealed significant differences between methods in HR estimation after decaffeinated coffee consumption ($p = 0.001$). Post-hoc analysis showed significant differences between EBA and CPDA ($p = 0.0006$), EBA and WTA ($p = 0.0003$), and EBA and pressure-gauge measurements ($p = 0.002$). Additional analyses confirmed significant effects of beverage type and method on HR ($p = 0.003$ for decaffeinated coffee; $p = 0.02$ for caffeinated coffee) and on CO after decaffeinated coffee ($p = 0.03$).

Conclusions: Overall, the wavelet-based approach demonstrated the greatest robustness to noise and the highest sensitivity to subtle physiological changes associated with caffeine intake. This work highlights the importance of selecting appropriate algorithms for remote cardiovascular monitoring and personalized healthcare and demonstrates their sensitivity to capture subtle changes induced by caffeine ingestion.

Keywords: impedance cardiography (ICG), signal processing, fiducial point detection, caffeine, hemodynamic parameters, stroke volume (SV), wavelet transform, extrema-based detection, biomedical signal analysis

Introduction

Impedance cardiography (ICG) is a non-invasive method for assessing cardiovascular function, enabling continuous monitoring of hemodynamic parameters such as cardiac output (CO), stroke volume (SV), and pulse wave velocity[1,2]. Due to its non-invasive nature, low cost, and ease of use, ICG represents an attractive alternative to more invasive diagnostic techniques, such as transesophageal echocardiography or cardiac catheterization[3,4]. CO and SV are calculated based on models using characteristic points on the ICG signal, i.e., fiducial points.

Currently, a major area of research in ICG focuses on developing accurate and reliable methods for detecting these landmark points in the signal. Precise identification of these fiducial points is crucial in cardiological diagnostics, especially for patients with heart failure, as it enables the calculation of key indicators such as CO and SV[5,6]. An additional and underexplored aspect is the effect to psychoactive substances such as caffeine on cardiovascular parameters recorded via ICG. Caffeine acts as a stimulant of the sympathetic nervous system, resulting in increased myocardial contractility, shortened pre-ejection period, and potential changes in signal amplitude and morphology[7,8].

© 2026 Authors This is an open access article licensed under the Creative Commons Attribution-NonCommercial-NoDerivs License (http://creativecommons.org/licenses/by-nc-nd/4.0/).

Authors' contribution: A – Research concept and design, B – Collection and/or assembly of data, C – Data analysis and interpretation, D – Writing the article, E – Critical revision of the article, F – Final approval of the article.

However, the automatic analysis of ICG signals faces numerous challenges, including the presence of noise, inter-individual variability, and morphological signal changes due to pathological conditions[9,10]. These factors significantly hinder the reliable detection of fiducial points and affect the accuracy of the final measurements. Another limiting factor is the lack of large, diverse, and well-annotated ICG databases, unlike electrocardiography (ECG), which benefits from multiple publicly available datasets. This hampers the development and validation of machine learning algorithms for ICG signal processing[11,12]. Therefore, our present and future research will allow us to increase the number of available datasets. In response to these limitations, researchers are developing advanced signal processing techniques, including wavelet-based methods, extremum detection, and time-domain fiducial point detection (CPDA)[13,14]. Such approaches are gaining importance, particularly in home-based monitoring contexts, with the use of smart bathroom scales or bed-integrated sensors[11,15].

In light of the above considerations, this study focuses on comparing analytical methods for the detection of reference points in the ICG signal. These approaches have been methodically grouped into three main classes to allow for a direct comparison of methods.

- Time-Domain Fiducial Point Detection (CPDA), as implemented in the 4hearts AMULET software[6];
- Extrema-Based Approach (EBA) which uses signal peaks within ECG-aligned time windows;
- Wavelet Transform Approach (WTA) which applies multiresolution signal decomposition to enhance signal clarity and facilitate point detection.

The categorization is presented in **Figure 1**.

In this study, three methods for analyzing impedance cardiography signals—CPDA, EBA, and WTA—were compared in terms of their effectiveness in detecting fiducial points and their sensitivity to hemodynamic changes induced by caffeine intake. All three methods are applied to physiological data collected before and after caffeine ingestion. The aim is to assess their relative performance and sensitivity to subtle hemodynamic changes, thereby identifying the most effective signal processing strategies for non-invasive cardiovascular monitoring under dynamic physiological conditions[12,16].

Materials and methods

Protocol

The impedance cardiography data were collected as part of an internal research project entitled "Study of the Effect of Caffeine on Activation Patterns Using rsfMRI in Young Non-Coffee Drinkers", conducted by the Łukasiewicz Research Network – Krakow Institute of Technology, Center for Biomedical Engineering. The physiological measurements were performed at the Military Institute of Aviation Medicine in Warsaw, Poland. The study involved a group of healthy volunteers without any diagnosed central nervous system or cardiovascular disorders. A total of 20 healthy subjects, 23.35 ± 2.82 years of age (between 20 and 28), who reported that they do not drink coffee at all or last drank it more than six months before the study, were recruited. Detailed demographic variables are included in **Table 1**. All procedures were performed on the same day, in the morning hours. The participants were asked to consume a light breakfast. The experimental protocol included the con-

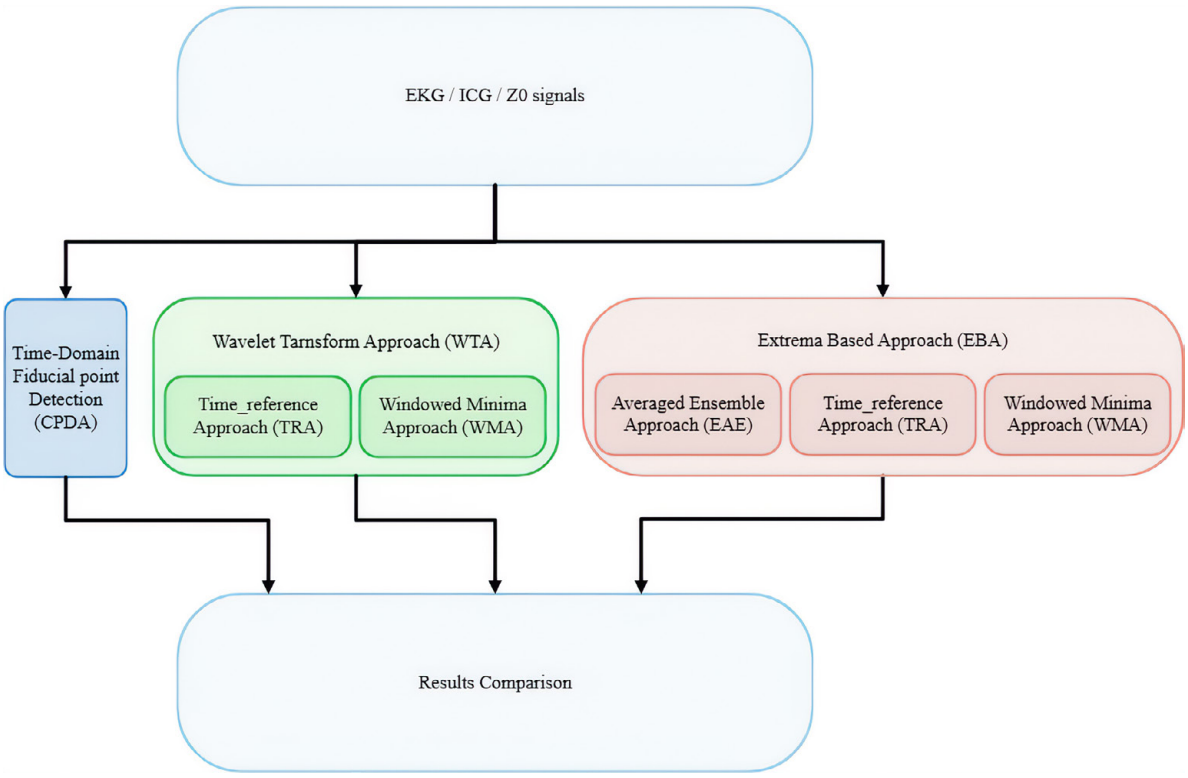


Figure 1. Architecture of fiducial point detection algorithms: CPDA, WTA, and EBA.

sumption of decaffeinated, and later caffeinated coffee, ICG assessment to monitor baseline cardiovascular parameters was performed 45min after consumption of decaffeinated coffee, and then 15 minutes after consumption of the caffeinated beverage. Caffeinated coffee contained around 80 mg of caffeine[17]. The participants were not informed which type of coffee they had consumed to eliminate any potential placebo effect. Surprisingly, the majority of participants did not recognize which cup contained caffeine, likely due to the stimulating effects of non-caffeine ingredients present in decaffeinated coffee. All participants were informed of the nature of the investigation, with a clear statement of the objective of the research and possible risk. They could withdraw at any time. The experimental protocol conformed to the principles presented in the Declaration of Helsinki and was approved by the ethical committee of the Military Institute of Aviation Medicine. Prior to the study, all the participants gave written informed consent to all procedures and personal data processing for scientific purposes. All data was defaced and anonymized before analyses.

Table 1. Demographic characteristics of study participants.

Variable	Men (n=13)	Women (n=7)	Total group (n=20)
Age [years]	22.46 ± 2.57	23.57 ± 3.10	22.85 ± 2.74
Body weight [kg]	77.08 ± 13.57	61.00 ± 8.21	71.45 ± 14.13
Height [cm]	180.92 ± 3.62	165.86 ± 5.67	175.65 ± 8.53

Data processing

In this study, three distinct analytical approaches were employed to highlight the differences in the analysis of the impedance cardiography signal. All methods are considered valid and are used in both clinical and research settings. One of the approaches has already been implemented in the 4hearts AMULET Software[6], where the algorithm is referred to as the Time-domain fiducial point detection approach (CPDA). This novel algorithm is based on a heuristic analysis of local slope changes, which provides high accuracy even in the presence of noise and signal variability.

The described method presents an effective approach for the accurate and reliable determination of characteristic points of the Impedance Cardiogram signal, which is crucial for assessing various hemodynamic parameters relevant to cardiological diagnostics, especially in patients with heart failure. The technique is implemented in the 4hearts AMULET software system for acquisition, visualization, and archiving of patient data, as well as real-time monitoring of these parameters. The signal processing methodology involves several key steps:

a) Signal Acquisition and ICG Derivation

The primary input signals are the Electrocardiogram and Bioimpedance (REO or Z), recorded simultaneously. The ICG signal, denoted as $\left(\frac{dZ}{dt}\right)$, is obtained by numerically differentiating the REO signal. The specific formula employed for this numerical differentiation is:

$$ICG[n] = 0.1 * f_s * (2 * REO[n+2] + REO[n+1] - \\ - REO[n-1] - 2 * REO[n-2])$$

where f_s represents the sampling frequency (e.g., 500 Hz), and REO[n] is the digitized bioimpedance waveform at sample 'n'.

b) Time Window Definition and ECG as Auxiliary Signal

The algorithm analyzes the impedance cardiography signal within a precisely defined temporal window T, whose length and position are determined based on previously identified fiducial points in the electrocardiography signal, specifically the R wave and the mean RR interval. This window is expressed as:

$$ICG[n] = 0.1 * f_s * (2 * REO[n+2] + REO[n+1] - \\ - REO[n-1] - 2 * REO[n-2])$$

where: T - analysis window for the impedance cardiography signal, R — position of the R wave in the electrocardiography signal, RR — mean RR interval, representing the average duration of the cardiac cycle, 7/20 and 13/20 — empirically determined coefficients defining how far before and after the R wave the analysis window extends, expressed as fractions of the RR interval

The ECG signal serves as an auxiliary reference for synchronizing and controlling the ICG analysis, which is particularly important for detecting arrhythmias that could complicate interpretation if relying solely on ICG.

Identification of characteristic points (B, C, X (**Figures 3,9,10**)):

- C point – identified as the maximum amplitude of the ICG signal within the defined time window T; physiologically, it corresponds to the peak aortic blood flow.
- B point – always preceding the C point, detected as the first positive peak occurring after the S wave in the third derivative of the ICG signal (REO_3). It typically appears after the QRS complex and before the onset of the T wave in the ECG. Physiologically, the B point marks the end of isovolumic contraction and the onset of the rapid ventricular ejection phase. Detection of this point is often challenging due to signal noise and morphological variability.
- X point – corresponding to the first minimum of the ICG signal occurring immediately after the termination of the T wave in the corresponding ECG signal. If the T wave cannot be reliably identified, the X point is defined as the first minimum in the ICG signal appearing after the systolic wave peak (REO) and after the C point. Physiologically, the X point indicates the end of ventricular contraction.

c) Hemodynamic Parameter Calculation

Once points B, C, and X are accurately identified, key hemodynamic parameters can be calculated. These include: $\left(\frac{dZ}{dt}\right)_{max}$ - this is the peak amplitude of the ICG systolic wave, defined as the difference between the values of points B and C. Left Ven-

tricular Ejection Time (LVET): This parameter represents the time interval between points B and X. These values are then used in established equations to calculate stroke volume and subsequently cardiac output . The Sramek–Bernstein equation is utilized for Stroke Volume calculation:

$$SV_{SB} = \frac{IW * 0.17 * H^3}{4.25 * \left(\frac{dZ}{dt}\right)_{max}} * LVET$$

where W is the subject's weight [kg], H is the subject's height [cm], $\left(\frac{dZ}{dt}\right)_{max}$ is the peak amplitude of the ICG signal, and LVET denotes the ventricular ejection time. IW (ideal weight) is calculated as: $IW = 0.534 * H - 17.36$ (for men) $IW = 0.534 * H - 27.36$ (for women).

Cardiac Output is then determined as the product of stroke volume and heart rate:

$$CO = SV_{SB} * HR$$

The effectiveness of this algorithm has been verified in clinical pilot studies, demonstrating a high correlation (r = 0.96) between cardiac output values obtained by the algorithm and those assessed by a medical expert. While some errors, particularly in B-point detection, can occur, especially in pathological recordings, the method is considered accurate enough for successful implementation in medical diagnostics, particularly for outpatient and telemedical applications where continuous, non-invasive monitoring is crucial

Extrema-Based Approach - EBA

The method is based on procedures proposed by Niroshana et al.[18]. A full analysis was performed in Matlab 2024a software with the use of two toolboxes: Signal Processing Toolbox and DSP System Toolbox. In the first step, the signals were filtered to reduce low-frequency and high-frequency artefacts including network artefacts (mainly 50 Hz). The signals were then subdivided into parts, each part covering a single cardiac cycle known as a heartbeat segment[18]; the parts were precisely synchronized with the occurrence of individual QRS complexes in the ECG trace. Each window included an interval of 200 ms before and 750 ms after the R wave, allowing the entire cardiac cycle to be captured. At the same time, ICG signals, including Z_0, were segmented into equal segments. This approach allowed accurate mapping of the cardiac cycle, along with the landmark morphological points of the signal (**Figure 2**) and those described below.

Filtration

As shown in the diagram (**Figure 2**), low-frequency artefacts associated with base drift were removed first, as well as high-frequency artefacts mainly from muscle activity and network artefacts (50 Hz). Bandpass filtering was used to eliminate interference for ECG, ICG and Z_0 signals. In particular, for the ECG and Z_0 signal, a bandpass Butterwoth 4th order filter was used in the frequency range from 0.5 to 40 Hz[19], which allowed the preservation of the signal's essential features while muting components that are harmful from the point of view of cardiac analysis ICG, however, uses bandpass filtering in the 0.5–30 Hz range[20]. Subsequently, the DC offset was removed from the signals, which unified the reference level of the signals and improved their comparability between different recordings.

Detection of QRS complexes

QRS complexes were detected with an algorithm using the Pan-Tompkins methodology[21], considered one of the most effective techniques for identifying R waves in the ECG signal, especially under the conditions of real-time signal analysis. The locations of R waveforms, corresponding to ventricular depolarization, served as key reference points for the temporal synchronization of the ECG signal. They were used to segment the data into so-called heartbeat segments, which provided a unified base for further processing and comparative analysis of cardiac cycles.

Averaged Ensemble Approach (AEA)

Signal segmentation

The ECG signal was divided into segments of 950 ms, covering 200 ms before and 750 ms after the onset of the R waveforms. In parallel, the impedance cardiography signals were also segmented, as well as the baseline Z impedance. From the last 15 complete segments, an averaged cardiac cycle was created, which made it possible to extract all the key stages of cardiac activity. In particular, it allowed unambiguous identification of landmark points B, C and X in the ICG signal, as well as the P, Q, S and T waveforms in the ECG signal (**Figure 3**). Point C was defined as the first local maximum (positive peak) in the ICG signal occurring after the end of the QRS complex, more precisely after the S waveform, but before the beginning of the T waveform in the ECG signal. This criterion makes it possible to distinguish a valid point C from potential artefacts or secondary fluctuations present in the signal.

Point B was defined as the moment of change in value, the derivative of chest impedance from negative to positive values, occurring immediately before the landmark point C[22]. Point X was determined as the first local minimum in the ICG signal appearing after point C. Correct identification of point X requires it to occur after the T waveform in the ICG signal. Taking into account the occurrence of the T waveform helps stabilize detection, especially for reduced SNR (Signal to Noise Ratio) in the impedance pathway[6].

Estimation of stroke volume and minute volume from an averaged cardiac cycle

To reduce the influence of noise and inter-systolic variability, an analysis based on an averaged cardiac cycle was performed. Based on the time of occurrence of points B and X, the mean left ventricular ejection time (LVET) was determined[23]. At the same time, the maximum rate of change in bioimpedance $\left(\frac{dZ}{dt}\right)_{max}$ [24] was determined, which is a key parameter in further hemodynamic analysis.

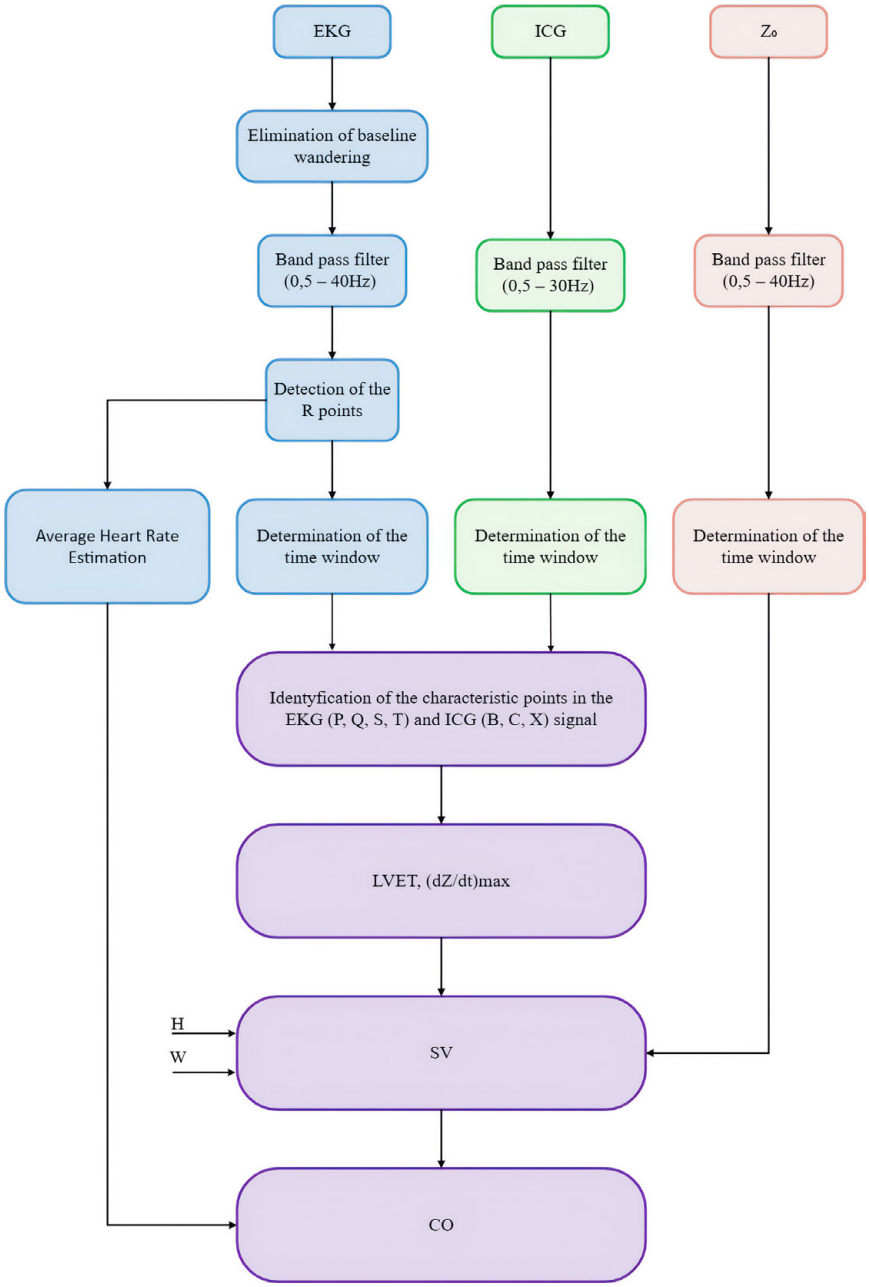


Figure 2. Block diagram of the algorithm determining the landmark points of the morphology of ECG and ICG signals in the middle complex.

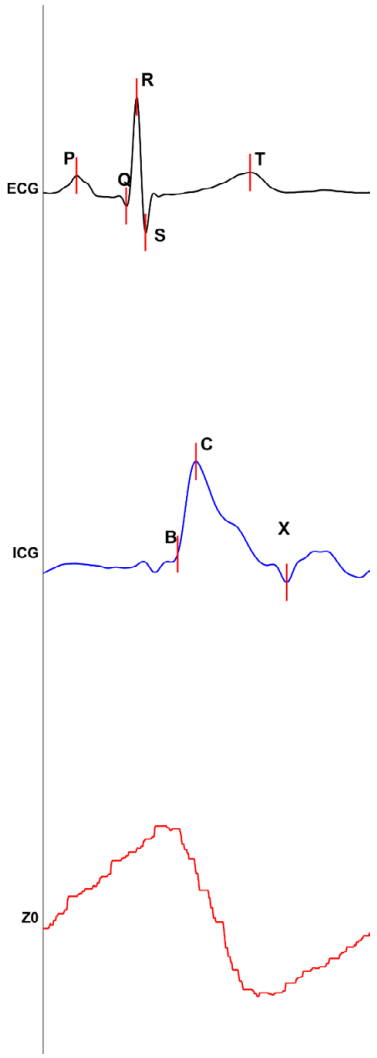


Figure 3. Electrocardiographic and Impedance Cardiographic signal landmark points in the Averaged Ensemble Approach (AEA). The R waveform of the ECG signal taken as the beginning of the cardiac cycle, point B – the beginning of blood ejection from the left ventricle, point C – the maximum of the Z impedance derivative after time in the cardiac cycle – dZ/dt_{max}, point X – the end of blood ejection from the left ventricle.

The value of cardiac stroke volume was estimated according to the relationship:

$$SV = \frac{\frac{W}{IW} * (0{,}17 * H)^3}{4{,}25 * Z_0} * \left(\frac{dZ}{dt}\right)_{max} * LVET$$

Where:

- W – patient body weight [kg],
- H – patient height [cm],
- IW – ideal weight taking into account sex = H (male 17,36, female 27,36)[25]

CO was calculated, which corresponds to the amount of blood flowing through the heart per minute[26].

$$CO = SV * HR$$

Time-Reference Approach (TRA) / Windowed Minima Approach (WMA)

QRS complexes were filtered and detected according to the AEA. Instead of segmentation, each of the last 15 complete cardiac cycles was analysed separately. Landmark points in the ECG and ICG signals were determined separately for each cycle. In the ICG signal, point C was designated identically to the AEA. Points B and X were determined in two ways (Time-Reference Approach (TRA) and Windowed Minima Approach (WMA)), in which respectively (**Figures 4, 5**):

- Points B and X are marked as minima occurring before and after the occurrence of point C, respectively;

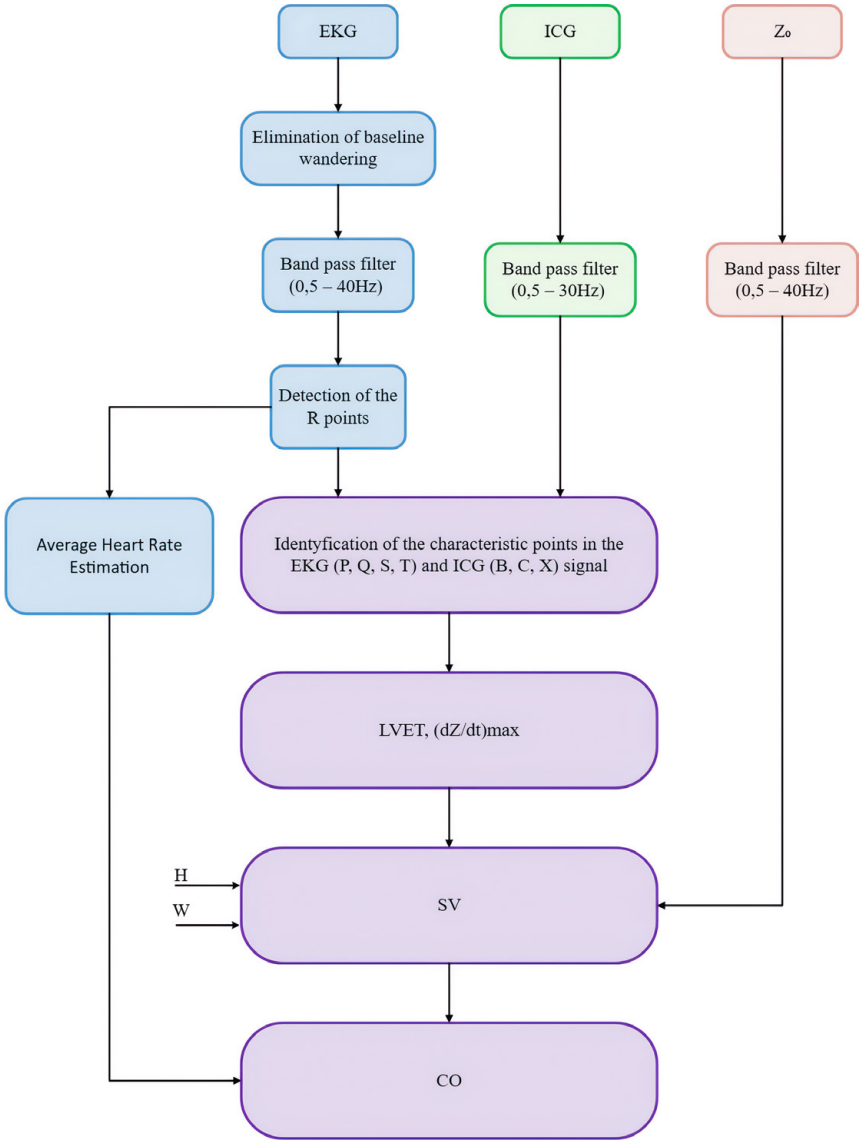


Figure 4 Block diagram of the algorithm determining the landmark points for the morphology of ECG and ICG signals for a single cardiac cycle.

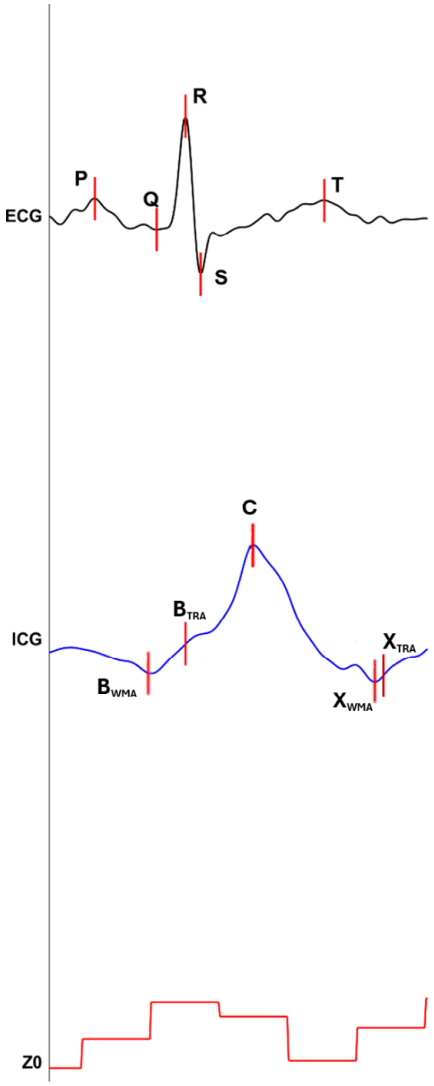


Figure 5 Comparison of medium complexes; two approaches: Time-Reference Approach (TRA) and Windowed Minima Approach (WMA).

- Points B were marked as the minimum occurring in no more than 80 ms before point C. Point X was marked as a minimum occurring between 120 ms and 250 ms after the occurrence of point C.

Heart rate (HR) calculations were made, LVET was estimated and $\left(\frac{dZ}{dt}\right)_{max}$ was determined. SV and CO calculations were made in the same way as in the AEA, as shown in **Figure 4**.

Wavelet Transform Approach – WTA

ICG signal filtration

The performance of various wavelet-based denoising techniques were evaluated to identify the most suitable wavelet for the filtration of the ICG signal. The wavelet-based denoising technique was chosen based on its established effectiveness in biomedical signal processing[27]. The analysis focuses on three prominent wavelet families – Daubechies, Symlet, and Coiflet – each tested across multiple wavelet orders.

The wavelet configurations that have been tested include:

- Daubechies family: db2, db4, db6, db8
- Symlet family: sym2, sym4, sym6, sym8
- Coiflet family: coif2, coif3, coif4, coif5

Daubechies wavelets are known for their compact support and orthogonality, making them highly effective for denoising non-stationary signals such as ICG[28]. Symlets, as modified Daubechies wavelets with improved symmetry, offer better phase preservation, which is crucial in cardiovascular signal analysis[29]. Coiflets, with vanishing moments for both scaling and wavelet functions, are particularly adept at capturing low-frequency trends and reducing baseline drift, common in ICG signals[27]. The evaluation criteria were based on three performance metrics such as signal-to-noise ratio (SNR), root mean square error (RMSE), percent root mean square difference (PRD). Within each family, the highest-performing wavelet orders were db8, sym8 and coif5, respectively. These wavelets demonstrated the highest SNR and the lowest RMSE and PRD within their respective families. In the final comparative analysis

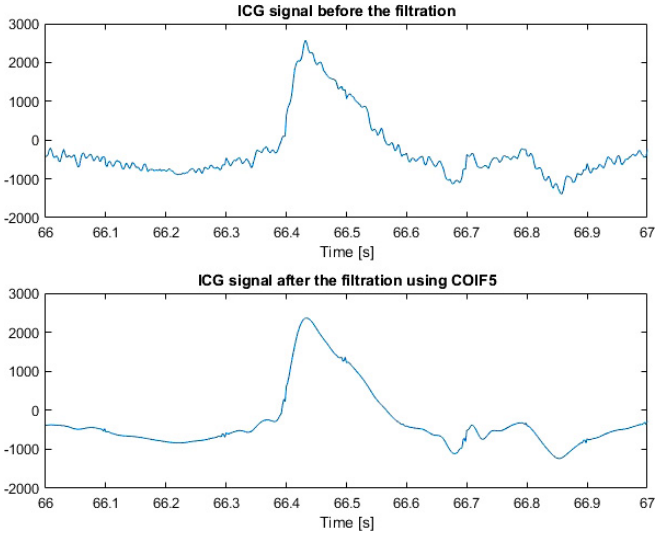


Figure 6. Comparison of the ICG signal before and after the filtration using COIF5

Table 2A. quantitative comparison of denoising performance across decomposition levels (L = 3–6) using the Coiflet5 (COIF5) wavelet applied to filter the ICG signal in the Wavelet Transform Approach (WTA)

Level	SNR (dB)	RMSE	PRD (%)
L = 3	26.07	0.00059	4.96
L = 4	28.15	0.00091	3.91
L = 5	28.13	0.00093	3.91
L = 6	28.12	0.00092	3.92

among the top-performing wavelets, Coiflet 5 (coif5) emerged as the most effective overall and was chosen for the whole set filtration method. The comparison of the ICG signal before and after the filtration using COIF5 can be seen in **Figure 6**. The wavelet decomposition level is a critical parameter influencing both denoising efficiency and morphological feature preservation in ICG signals. For this purpose, the decomposition levels ranging from L = 3 to L = 6 were evaluated simultaneously to determine the optimal level for signal analysis. **Table 2** presents the quantitative evaluation of denoising performance across different wavelet decomposition levels (L = 3–6). Decomposition at L = 3 resulted in the lowest signal-to-noise ratio (26.07 dB) and the highest PRD (4.96%), indicating insufficient noise suppression. Increasing the decomposition level to L = 4 led to a substantial improvement in denoising performance, with the SNR increasing to 28.15 dB and the PRD decreasing to 3.91%. Further increases in the decomposition level (L = 5 and L = 6) did not yield additional improvements. Overall, L = 4 provided the optimal trade-off between noise reduction and signal fidelity, achieving the highest SNR and the lowest PRD among all tested levels. Therefore, a decomposition level of L = 4 was selected for subsequent analyses.

ICG signal decomposition

The ICG signal was decomposed using the Maximal Overlap Discrete Wavelet Transform (MODWT) with the coif5 wavelet. Decomposition was performed up to six levels, and the detail coefficients at levels 4, 5, and 6 (denoted as D4, D5, and D6) were selected for further analysis based on their ability to preserve the morphological features of the ICG waveform (**Figure 7**).

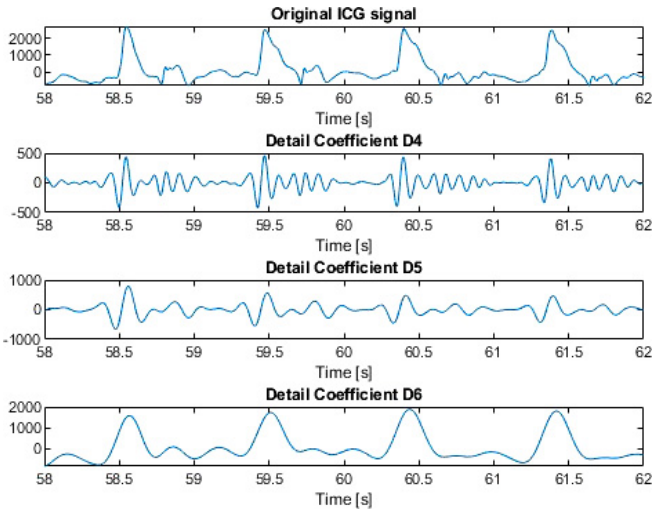


Figure 7. The original ICG signal and the detail coefficients D4, D5, and D6 obtained from MODWT using the coif5 wavelet

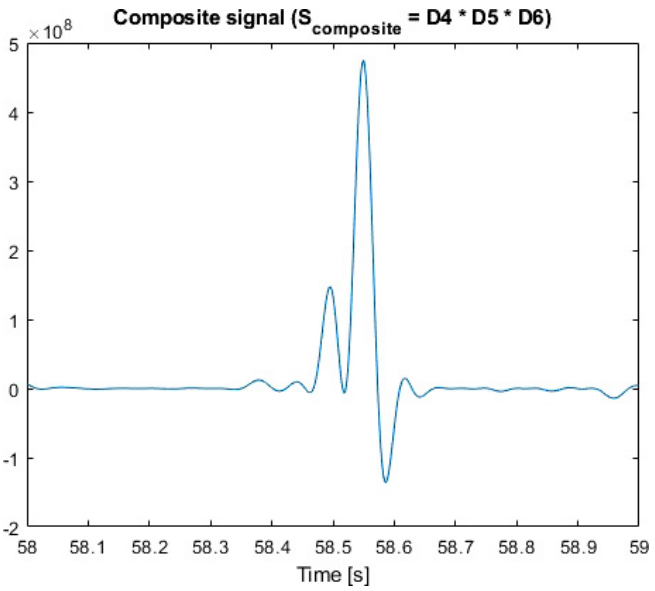


Figure 8. The composite signal $S_{composite}$ = D4·D5·D6, which serves as the basis for fiducial point detection for the first and second approach.

A composite signal was constructed by taking the pointwise product of the selected detail coefficients:

$$S_{composite}=D4\cdot D5\cdot D6$$

This composite signal was used as the basis for fiducial point detection (**Figure 8**).

BCX Detection – first approach (TRA)

The detection process was applied on a per-ensemble basis, permitting greater adaptability to beat-to-beat variability (**Figure 9**).

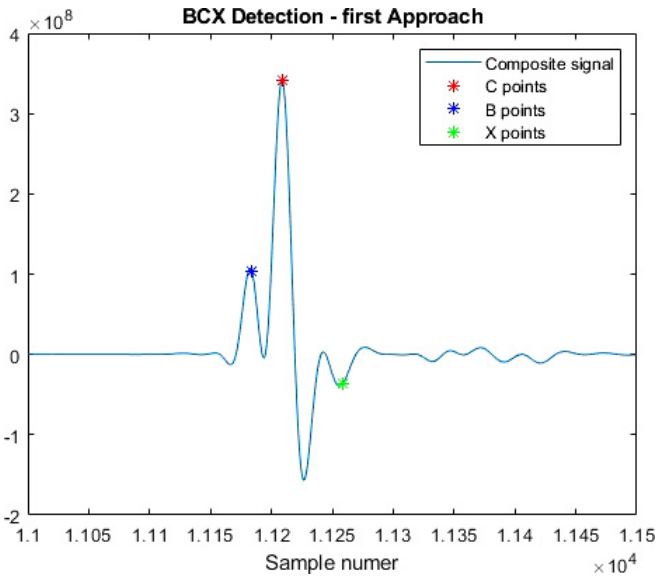


Figure 9. BCX Detection – first approach.

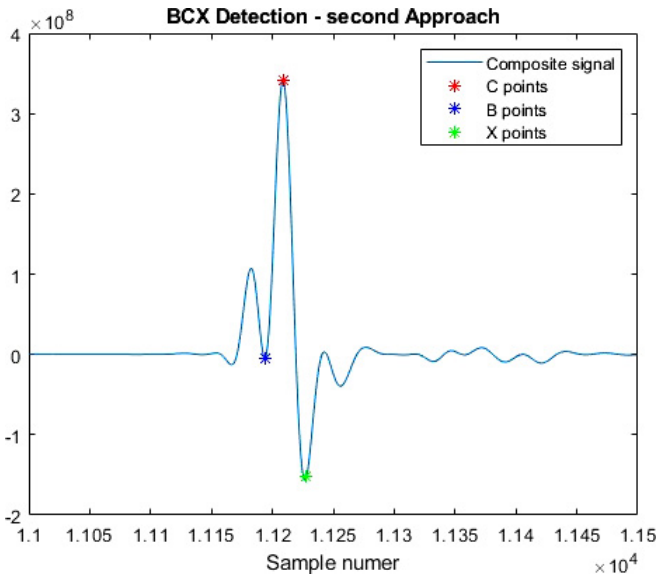


Figure 10. BCX Detection – second approach.

- Point C Detection:
  By analogy to the first approach, point C was defined as the maximum of the composite signal within each ensemble.
- Point B Detection:
  Point B was identified by searching for a local maximum in the composite signal within an 80 ms window preceding point C. This inversion-based method enhances the visibility of subtle minima in the original signal.
- Point X Detection:

Point X was located as the local minimum in a fixed interval of: [C+100 ms, C+200 ms]

BCX Detection – second approach (WMA)

As in the previous approach, the detection process was applied on a per-ensemble basis (**Figure 10**).

- Point C Detection:
  Point C was defined as the global maximum of the composite signal $S_{composite}$. To ensure physiological plausibility and avoid false positives, a minimum inter-peak interval of 600 ms was enforced between successive points C.
- Point B Detection:
  Point B was identified as the local minimum immediately preceding point C in the composite signal. This approach did not impose a fixed temporal window, relying instead on the morphological structure of the waveform.
- Point X Detection:
  Point X was determined by locating a local minimum within a dynamic interval defined as:

$$[C+0.1\cdot CC_{mean}, C+0.5\cdot CC_{mean}]$$

  where CC_{mean} represents the average cardiac cycle duration.

Blood pressure was additionally obtained with an automated blood pressure monitor.

Statistical analysis

Statistical analysis was performed using Statistica 13.3 software. After checking the normal distribution (tested with the Shapiro–Wilk test), analysis of variance with repeated measures was applied. Mauchly's test of sphericity was included as part of the procedure. Post-hoc LSD (*Least Significant Difference)* tests were performed for statistically significant parameters. The level of statistical significance was set at $p < 0.05$. Linear regression and Pearson's correlation coefficient (r) were used. For the Time-Reference Approach (TRA) HR method, ANOVA with repeated measures was performed. Post-hoc LSD tests were performed, which allowed for detecting differences between parameters estimated by all the described models (CPDA, EBA, WTA).

Statistical analysis without and with sex breakdown

1. Stroke volume (after consumption of DECAF coffee) was larger among males than females, regardless of method of determination (all $p<0.04$). **Figure 11** and **Tables 3-4** show the average values of HR, SV and CO after drinking decaffeinated coffee and regular coffee, determined by different methods, as a function of sex, no statistically significant differences. However, we noticed interesting trends between the sexes. As for the heart rate, after drinking both decaffeinated coffee and regular coffee, women had higher heart rates than men, regardless of the processing method. As for the stroke volume, men had higher values than women after drinking coffee (see **Table 3,4**). Cardiac output was similar, with the exception of the values for the WTA method. For both stroke volume and cardiac output, men experienced an increase in values between the different methods for determining values, here the CPDA method yielded the highest CO and SV for women.

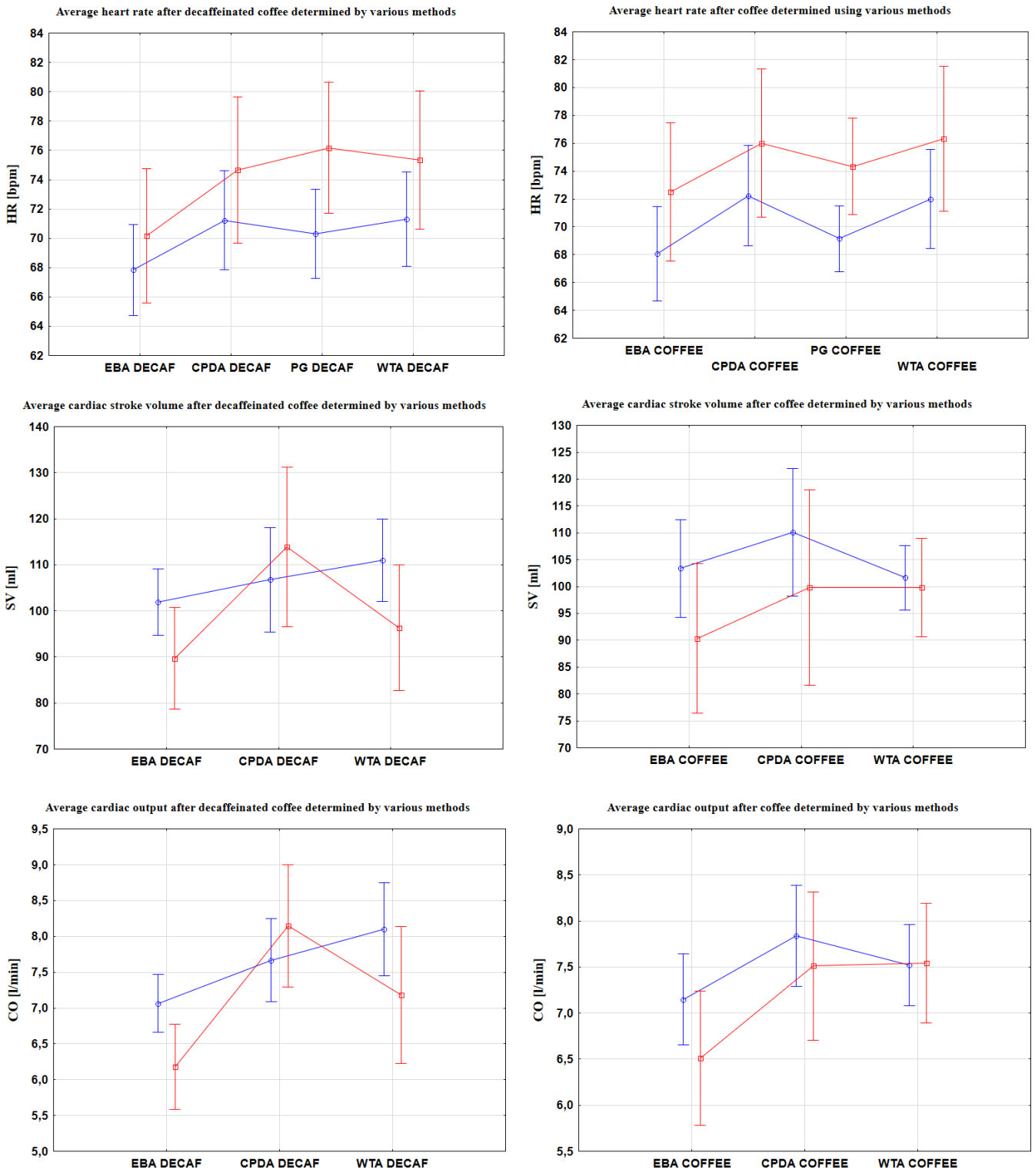


Figure 11. Average HR-heart reate, SV-stroke volume and CO-cardiac output after drinking decaffeinated (left) and regular coffee (right), determined by different methods, divided by sex (where the blue line with circles: male sex, the red line with squares: female sex), no statistically significant differences.

2. Differences between methods used for parameter determination (without gender-based division).

Figures 12, 13 show how the CO and SV parameters, determined using the three methods, change after coffee. We can see that the WTA method has the smallest dispersion in both parameters, which is confirmed by the lowest standard deviation values compared to the other two methods. In the case of CO, the standard deviations are for EBA ±1.76, CPDA ±1.92 and WTA ±1.54, respectively. In the case of SV, the standard deviations are for EBA ±33.77, CPDA ±43.59 and WTA ±21.82, respectively.

For the Time-Reference Approach method, ANOVA with repeated measures was performed. The analysis revealed statistically significant differences regardless of sex for HR after drinking decaffeinated coffee, p = 0.001 (**Figure 14**). Additionally, a post-hoc LSD test performed for HR after the decaf-

Table 3. Mean heart rate (HR) values and standard deviations for females and males obtained with Extrema-Based Approach (EBA), Time-Domain Fiducial Point Detection (CPDA), and Wavelet Transform Approach (WTA) methods, and compared to blood-pressure gauge (PG) readouts, after both decaffeianed and coffeinated beverage.

		Processing Method			
		EBA	CPDA	WTA	PG
Decaff	Female	70.17±4.58	74.67±4.99	75.33±4.73	76.17±4.47
	Male	67.85±3.11	71.23±3.39	71.310±3.21	70.31±3.03
Caffeine	Female	72.5±4.98	76.0±5.32	76.33±5.21	74.33±3.47
	Male	68.08±3.38	72.23±3.61	72.0±3.54	69.15±2.36

Table 4. Mean stroke volume (SV) values and standard deviations for females and males obtained with Extrema-Based Approach (EBA), Time-Domain Fiducial Point Detection (CPDA), and Wavelet Transform Approach (WTA) methods, and compared to blood-pressure gauge (PG) readouts, after both decaffeinated and caffeinated beverage.

		Processing Method		
		EBA	CPDA	WTA
Caffeine	Female	90.33±13.93	99.83±18.17	99.83±9.14
	Male	103.36±9.12	110.07±11.9	101.64±5.99
Decaff	Female	89.67±11.03	113.83±17.33	96.33±13.67
	Male	101.86±7.22	106.79±11.34	111.00±8.95

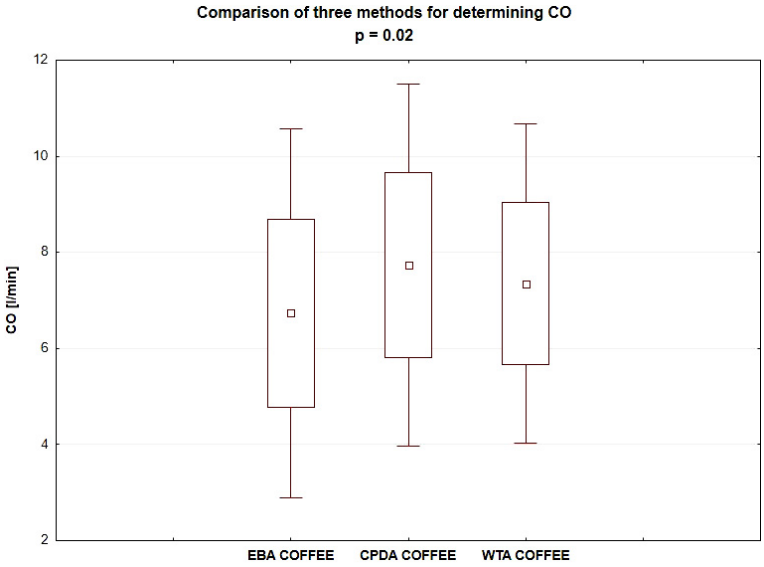


Figure 12. Comparison of three methods for determining cardiac output (CO) – after coffee.

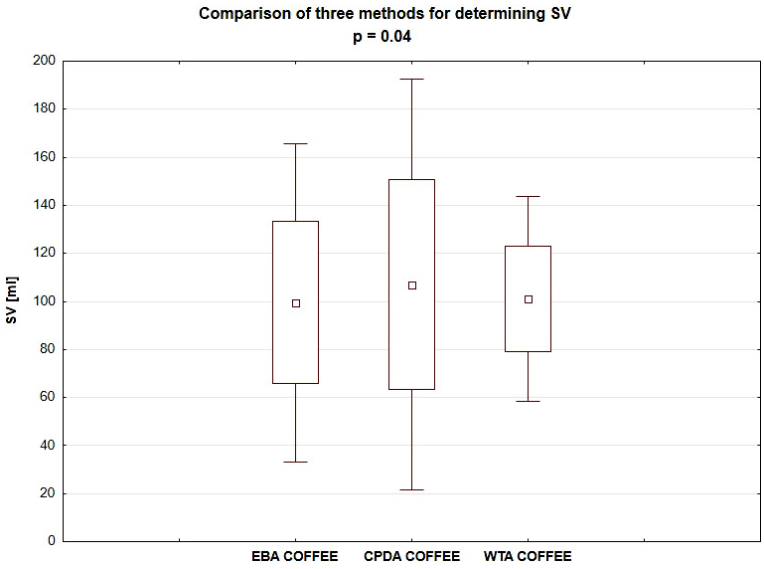


Figure 13. Comparison of three methods for determining stroke volume (SV) – after coffee.

feinated drink was consumed showed statistically significant differences between HR obtained with EBA and CPDA methods p = 0.0006, EBA method and readouts from the blood-pressure gauge (PG) p = 0.002, as well as results from EBA and WTA methods p = 0.0003.

3. Effect of decaffeinated and regular coffee consumption

For the WMA method, ANOVA with repeated measures evaluated the effects of caffeine consumption. The analysis revealed statistically significant differences regardless of sex for HR after drinking decaffeinated coffee p = 0.003 and HR after drinking regular coffee p = 0.02.

Additionally, post-hoc LSD tests were performed, which made it possible to find differences between the results obtained with evaluated methods. After drinking the decaffeinated drink, the post-hoc LSD test for showed statistically significant differences between results obtained with EBA and CPDA method p = 0.003, EBA results and PG readouts p = 0.004, results of EBA and WTA methods p = 0.001. The post-hoc LSD test for HR after drinking regular coffee showed statistically significant differences between results obtained with EBA and CPDA methods p = 0.005, as well results obtained with EBA and WTA methods p = 0.006.

ANOVA with repeated measures analysis of the averaged data was performed. The analysis revealed statistically significant differences regardless of sex for HR after drinking the decaffeinated p = 0.004, HR after drinking coffee p = 0.021, and CO after drinking the decaffeinated drink p = 0.03 (**Figures 14, 15**). The post-hoc analysis for HR after consuming a decaffeinated beverage demonstrated statistically significant differences between EBA and CPDA methods (p = 0.004), EBA and pressure gauge (PG) p = 0.005, as well as EBA and WTA p = 0.002. After drinking regular coffee, HR was significantly different EBA and CPDA methods (p = 0.004), as well as EBA and WTA (p = 0.005). Again, after consuming decaffeinated coffee, CO was significantly different between EBA and CPDA methods (p = 0.03), as well as EBA and WTA methods (p = 0.03).

Please note that EBA yields a result significantly different from others.

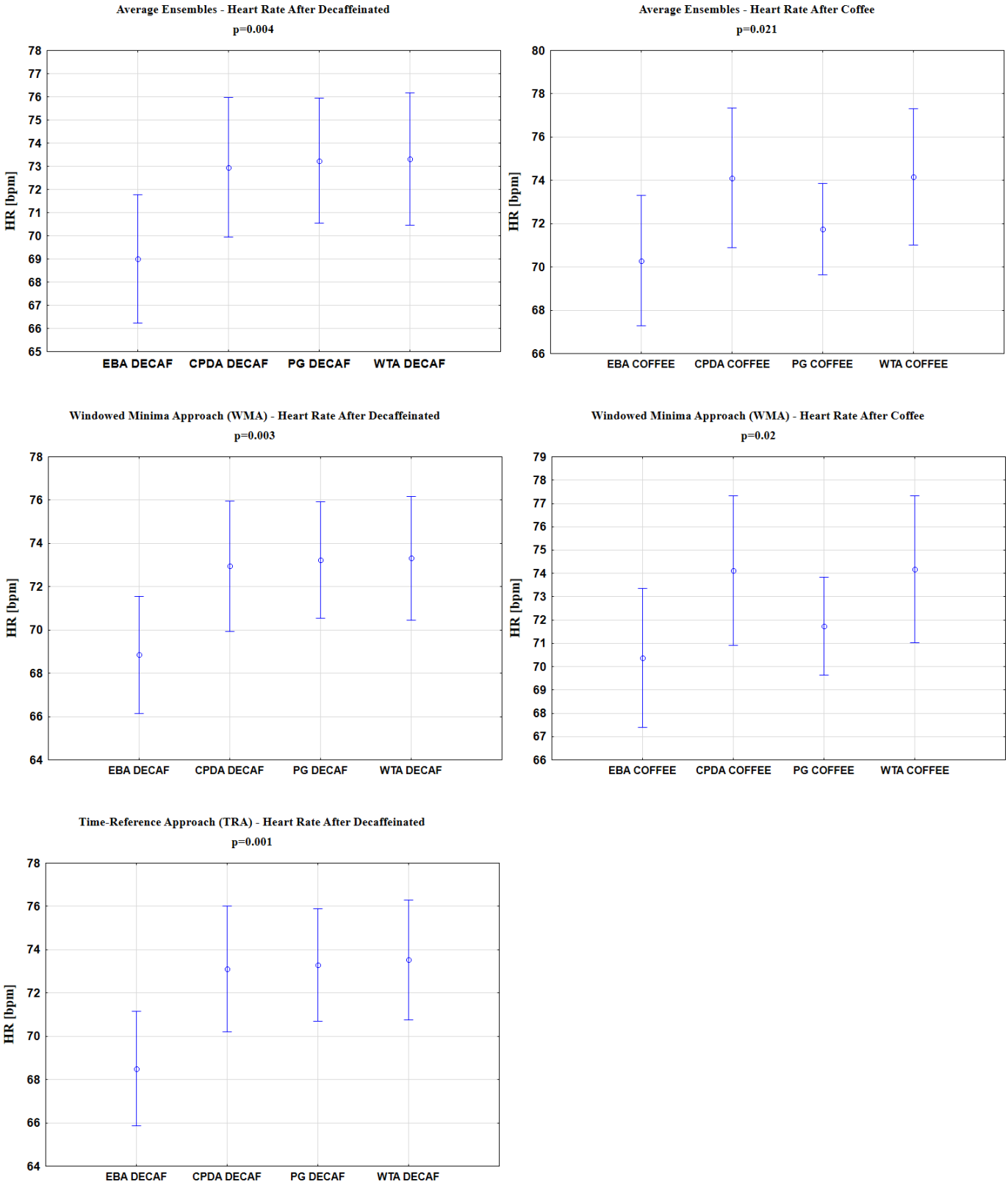


Figure 14. HR after drinking regular and decaffeinated coffee, where PG – pressure gauge, DECAF – decaffeinated coffee, COFFEE – caffeinated (regular) coffee.

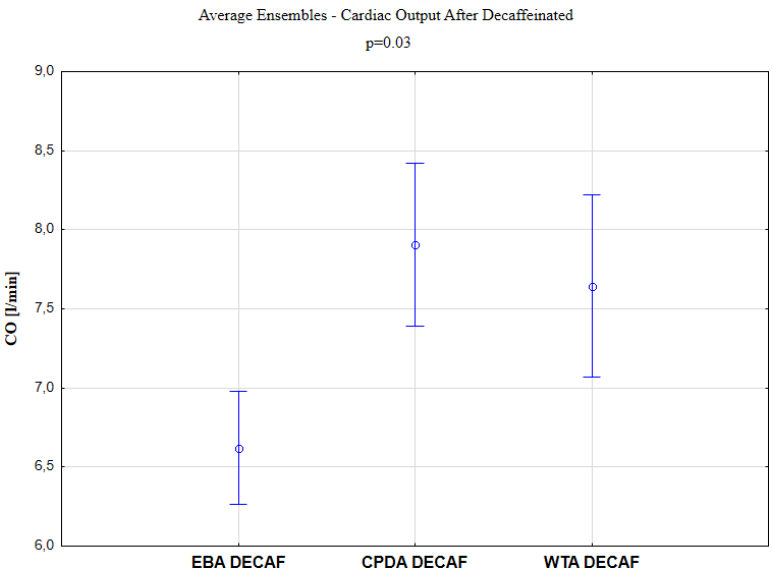


Figure 15. Average cardiac output (CO) after drinking decaffeinated coffee.

ICG Methods Comparison

Comparing heart-rate measurements obtained with PG with measures obtained using WTA analysis of the ICG signal, a visible trend suggests proportional bias indicating that measurement differences increase with higher mean values (**Figure 14**). Such proportional errors may undermine the reliability of these methods for clinical or research purposes when precise agreement is critical. Even small discrepancies in signal interpretation can lead to divergent conclusions, especially in contexts where clinical accuracy is crucial. Nonetheless, despite the observed bias in certain method pairs, not all combinations exhibit this limitation. The Bland-Altman plots in **Figure 16** illustrate pairs of heart rate measurement methods. We can see that the line showing the average difference between methods is close to 0 for the following method pairs: EBA and PG, as well as CPDA and WTA after caffeinated coffee consumption. On the other hand, after decaffeinated coffee was consumed CPDA results were consistent with PG, CPDA with WTA, as well as PG and WTA. This indicates that these methods produce similar results for a given type of coffee.

Figure 17 demonstrates a qualitative comparison of three approaches to ICG signal analysis: CPDA, EBA, and WTA. CPDA and EBA received the highest accuracy rating (★★★★), while WTA was not rated in this category. Regarding sensitivity to noise, WTA showed the highest responsiveness (▲▲), WTA moderate (▲), and CPDA (▲). In terms of application, CPDA and EBA are classified as clinical methods, whereas WTA is considered suitable for home-based use.

Figure 18 shows correlations between the body mass index (BMI), body weight and blood pressure and cardiac stroke volume determined by various methods. The correlation values were determined for "body weight" with "SV" WTA DECAF r = 0.62, "BMI" with "SV" WTA DECAF r = 0.61, "BMI" with "SV" CPDA DECAF (WMA) r = 0.58, "body weight" with "SV" CPDA DECAF (WMA) r = 0.52, "BMI" with "SV" CPDA DECAF (TRA) r = 0.51, "BMI" with "SV" CPDA after drinking decaf (Average) r = 0.58, and "BP1 DECAF diastolic with "SV" WTA DECAF r = 0.59. These findings suggest that individuals with higher body mass and BMI tend to exhibit higher stroke volume values. This relationship is physiologically plausible, as greater body size is typically associated with increased metabolic demand and circulating blood volume, which may lead to higher cardiac preload and consequently higher stroke volume through the Frank–Starling mechanism[30]. Previous cardiovascular studies have demonstrated that cardiac output and stroke volume scale with body size and body composition, reflecting structural and functional adaptation of the cardiovascular system[31,32]. It should be noted, however, that BMI is an indirect measure of adiposity and does not distinguish between fat mass and lean body mass. Therefore, the observed associations may partly reflect differences in body composition, cardiovascular fitness, or cardiac structural remodeling rather than adiposity alone[33]. The moderate strength of the correlations further indicates that stroke volume variability is influenced by multiple physiological determinants, including autonomic regulation, vascular compliance, and ventricular contractility. The persistence of these relationships after decaffeinated coffee intake suggests that they are primarily driven by underlying physiological characteristics rather than acute pharmacological stimulation. Unlike caffeine-containing beverages, decaffeinated coffee is not expected to substantially increase sympathetic activation or systemic vascular resistance, which may explain the relative stability of the observed associations across experimental conditions[34]. The positive correlation between stroke volume and diastolic blood pressure may reflect the interaction between cardiac output and peripheral vascular resistance. Higher stroke volume may contribute to greater arterial filling and maintenance of diastolic pressure, particularly in individuals with preserved vascular compliance. However, given the observational nature of the present analysis, causal interpretation should be made with caution.

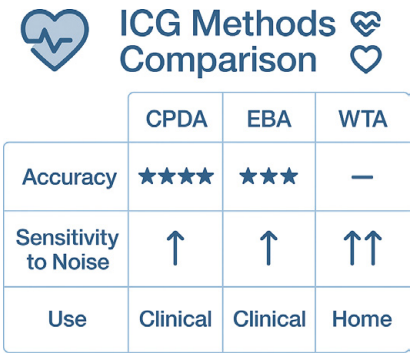


Figure 17. Comparison of three ICG signal analysis methods (CPDA, EBA, WTA) in terms of accuracy, noise sensitivity, and potential application. Stars (★) indicate the relative accuracy of each ICG method, with a higher number of stars representing greater accuracy compared to the other methods. A dash (—) indicates that accuracy was not assessed or is not directly comparable. Arrows (↑) denote sensitivity to noise, where a higher number of arrows reflects greater susceptibility of the method to signal noise.

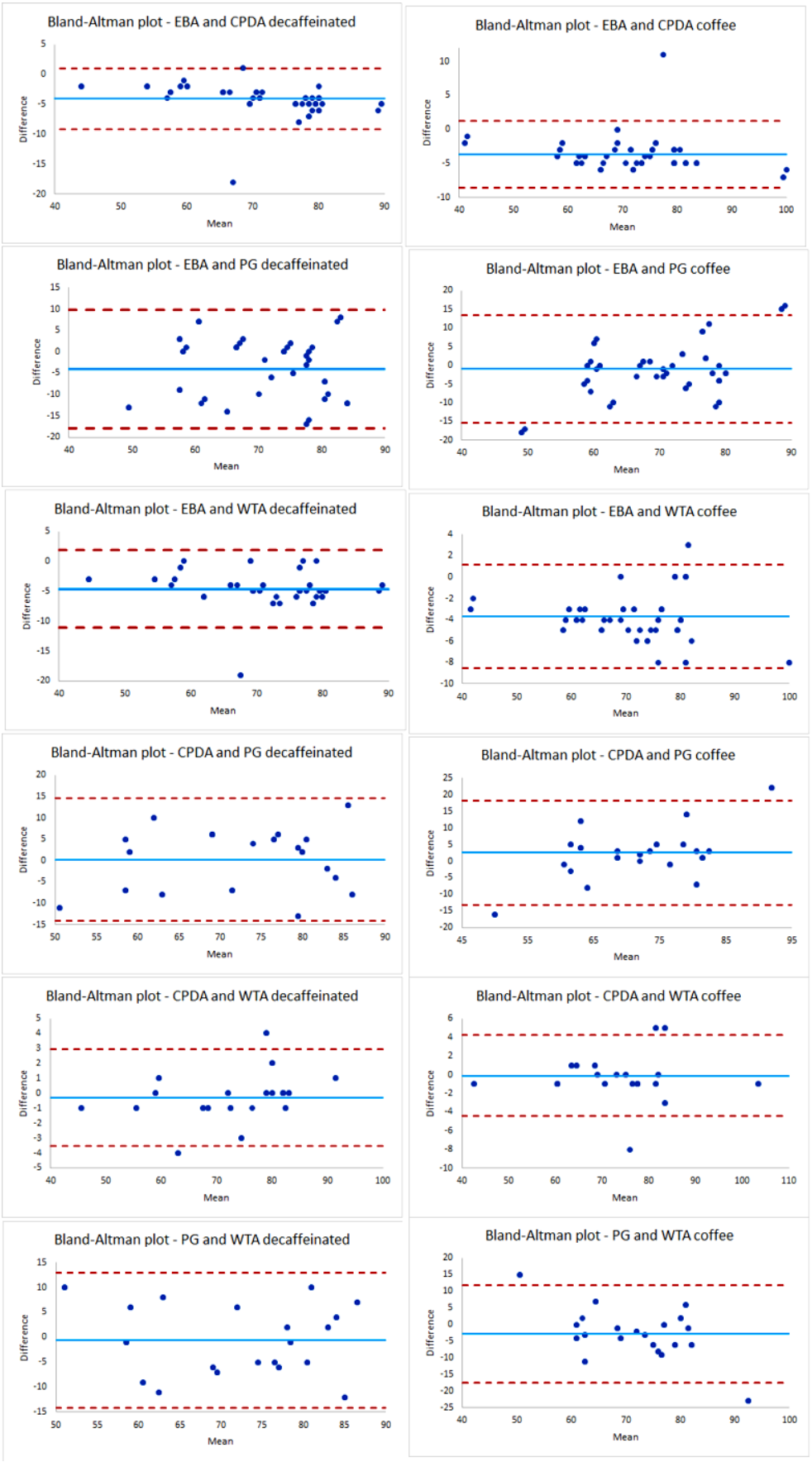


Figure 16. Bland-Altman plots present the differences between pairs of heart rate measurement methods in relation to their mean values. The red dashed lines represent the limits of agreement (±1.96 SD), while the solid blue line indicates the average difference (bias) between the methods. For most comparisons such as EBA and PG (coffee), CPDA and PG (decaffeinated), CPDA and WTA (both coffee and decaffeinated), and PG and WTA (decaffeinated), the mean difference remains close to zero, suggesting a high level of measurement agreement. The observed deviations fall within acceptable limits, indicating that these methods may be used interchangeably for specific types of coffee.

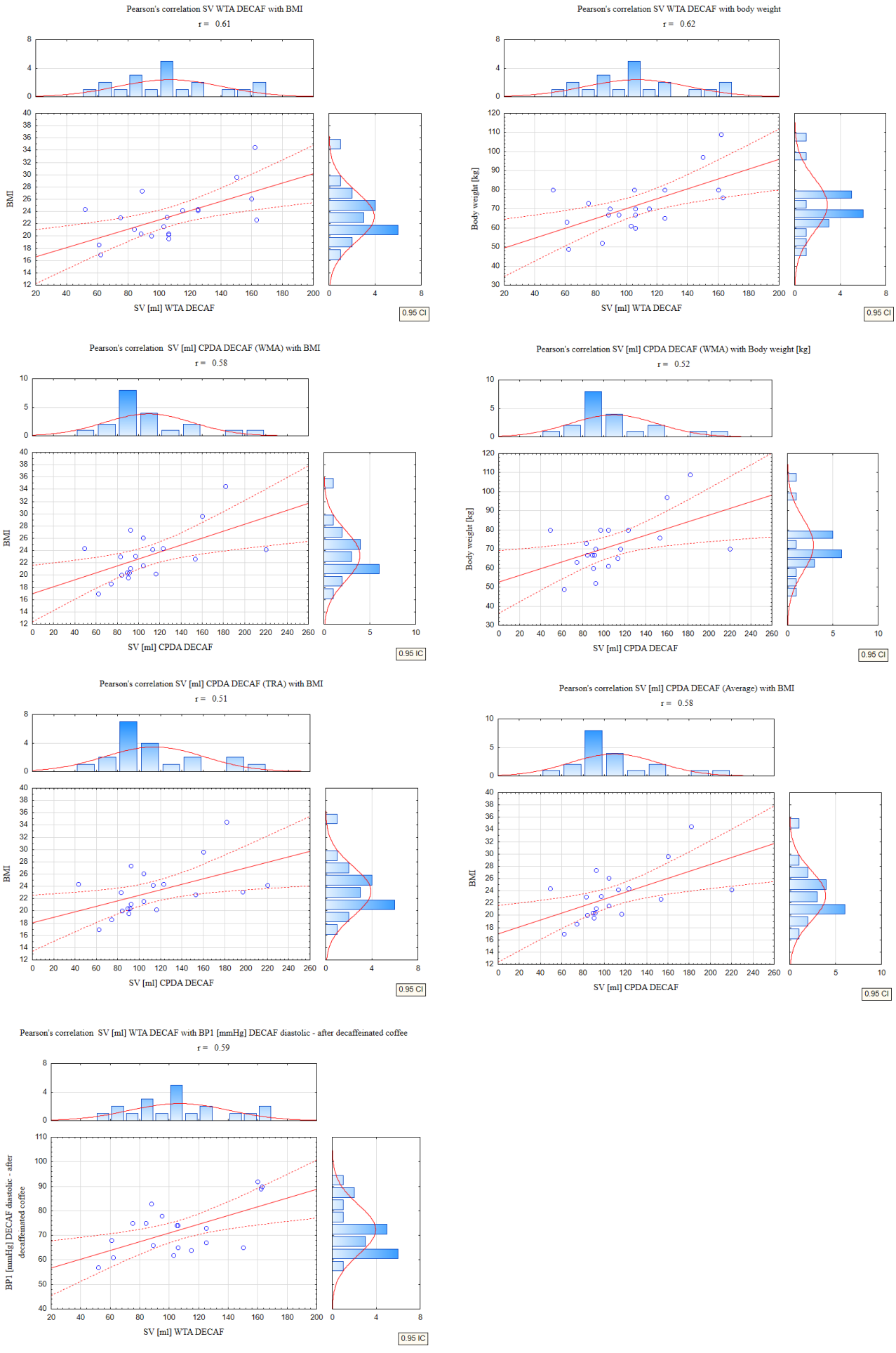


Figure 18. Heart stroke volume correlations plots.

Discussion

The primary objective of this study was to evaluate the effectiveness of different signal processing approaches in detecting key fiducial points within the impedance cardiography waveform, and to assess their sensitivity in identifying subtle cardiovascular changes following caffeine ingestion. The comparative analysis included three distinct methods: the Time-Domain Fiducial Point Detection Approach, the Extrema-Based Approach, and the Wavelet Transform Approach.

Our findings reveal notable differences in the stability and precision of landmark point detection between the methods. Each algorithm displayed unique advantages depending on the nature of the signal and the degree of noise present. In particular, Wavelet Transform Approach manifests its potential applicability in clinical monitoring[35,36].

The results obtained in our study show clear differences between methods for detecting landmark points in the ICG signal, both in terms of measurement stability and sensitivity to caffeine-induced hemodynamic changes. In particular, the wavelet transform-based method proved to be more robust to noise and better at differentiating between SV and HR changes, which is consistent with previous reports on the effectiveness of wavelet filtering in the analysis of cardiac signals[37]. The study[27] compared classical time-domain approaches with wavelet transforms for the ICG signal and showed that methods based on multiresolution decomposition offer higher accuracy of points B and X location and are less sensitive to artefacts. Our observations support these findings, especially in the context of cardiac cycle averaging and SV assessment.

Our associations of CV and CO with sex and BMI validate our them physiologically. Evans

Evans et al (2017) described that body weight, height and body surface area are correlated with changes in SV, CO and blood pressure, both in the supine and standing positions[38]. Our observations resonate with this state of the art; higher SV and CO values in subjects with greater weight and height confirm that it is worth taking these factors into account during hemodynamic analyses. In addition, de Simone et al. (1997) showed that excessive body weight significantly increases SV and CO in a normotensive population, which coincides with the observed effects of BMI on stroke volume and circulatory support in our results[31].

Similar findings were reported by Pale et al. (2021), who introduced ReBeatICG – a real-time, low-complexity algorithm for beat-to-beat delineation of the impedance cardiogram. Their work demonstrated that the choice of the fiducial point detection method significantly impacts the accuracy of hemodynamic parameter estimation (e.g. HR, LVET, IVRT), with discrepancies of up to several milliseconds. This highlights the necessity of standardizing fiducial point identification techniques to ensure the consistency and reproducibility of cardiovascular signal analysis results[39]. Previous validation studies of B-point detection algorithms have similarly demonstrated that different computational approaches may yield substantially different estimates of systolic time intervals, emphasizing the importance of algorithm selection and validation against visual scoring procedures[40–42].

Regarding caffeine's impact, our results align with Almeida et al. (2024), whose systematic review and meta-analysis (10 RCTs, caffeine doses 2.1–6.0 mg/kg) found that post-exercise caffeine intake does *not* significantly change HRV recovery indices (RMSSD, HF power) compared to placebo – suggesting that, in healthy active adults, caffeine's effect on cardiac autonomic modulation is minimal[43]. Furthermore, a controlled trial in strength training (300 mg caffeine, 45 min before exercise) reported that acute caffeine intake delays HRV recovery and other cardiovascular recovery metrics post-exercise, indicating a transient HR impact that may not be persistent[44]. In summary, caffeine appears to primarily affect the heart rate with transient effects on HRV post-exercise, while its influence on stroke volume is ambiguous. Moreover, discrepancies between signal processing methods – particularly between EBA and WTA – can either obscure or exaggerate these effects depending on algorithm sensitivity and filtering choices. These findings highlight the importance of method selection based on both the sample type and the intended application, as not all methods yield consistent results across different conditions. These observations underscore the complexity of comparing different signal processing methods, in particular when individual biases or proportional errors emerge. Furthermore, the observed variability in algorithmic sensitivity underscores the complexity of interpreting ICG signals in real-world scenarios. These findings not only validate the importance of selecting appropriate signal processing techniques but also emphasize the broader implications of such choices in clinical and research settings.

This topic fits into the broader context of the growing importance of non-invasive methods for monitoring cardiovascular function and the personalization of healthcare. The analysis of changes in the ICG signal following caffeine ingestion represents an important step toward a better understanding of the impact of commonly consumed psychoactive substances on hemodynamic parameters. The use of comparative approaches to fiducial point detection, aimed at optimizing signal quality, not only enables the evaluation of the effectiveness of various algorithms, but also highlights directions for further improvements in the automation of the ICG analysis. Such an approach is particularly relevant in the context of the development of wearable technologies and telemedicine systems, increasingly used in home settings. Through continuous improvement of signal processing and interpretation methods, it becomes possible to create more sensitive, accurate, and contextually adaptive diagnostic tools. In the long term, this can significantly expand the potential of preventive and AI-assisted medicine, leading to faster identification of cardiovascular irregularities and better tailoring of therapies to the individual needs of patients.

Limitation

Several limitations of the present study should be acknowledged.

- First, the caffeine dose (80 mg) was administered as a fixed amount rather than normalized to body weight (mg/kg). This approach was chosen to reflect a realistic and ecologically valid caffeine exposure comparable to the caffeine content of a standard cup of coffee. The effects of caffeine ingestion are genetically - driven. On the opposite, we were interested to induce a range of reaction strengths in order to perform valid correlational analyses. Additionally, the study focused on young adults with very low/zero habitual caffeine intake, for whom even a moderate absolute dose of caffeine may elicit pronounced physiological effects[45,46].
- Second, the study sample was relatively small (N = 20) and consisted exclusively of healthy young adults aged 20–28 years. This homogeneous sample was intentionally selected to reduce confounding factors related to age, health status, and habitual caffeine consumption. Although the limited sample size and narrow age range reduce the generalizability of the findings to broader populations, including older individuals or habitual caffeine consumers, it is a novel study of a population not consuming caffeinated beverages.
- Finally, a potential gender imbalance may have further influenced the results, as sex-related differences in caffeine metabolism and sensitivity have been reported. Due to the limited sample size, sex-specific analyses were not feasible and should be addressed in future studies with larger and more balanced cohorts.

Conclusion

The Wavelet Transform Approach demonstrated the highest precision and measurement stability, showing strong resistance to signal noise and providing the most physiologically consistent estimates of stroke volume and cardiac output. While the CPDA method is well established in clinical practice, it proved more susceptible to signal variability, which may limit its applicability in home-based or low-quality signal environments. The EBA method, based on extrema detection, showed the greatest variability and the lowest sensitivity to subtle physiological changes, although its simplicity may be advantageous in low-complexity systems. Discrepancies between methods in SV and CO values reached several liters per minute, underscoring the need for standardization of ICG signal analysis algorithms. Additionally, individual characteristics such as body weight and BMI significantly influenced hemodynamic parameters, highlighting the importance of personalized algorithm design in future clinical and telemedicine applications, as well as points to sensitivity of the methods to capture subtle changes in hemodynamics, as those observed in our study. Given the observed variability and the influence of individual physiological characteristics, future studies should aim to expand the study cohort, with particular emphasis on increasing the number of female participants, to validate these findings across a more diverse population and explore potential sex-specific patterns in ICG-derived cardiovascular parameters.

Statement of Significance

Problem or Issue: Accurate detection of fiducial points in impedance cardiography (ICG) signals is critical for reliable cardiovascular monitoring, especially under dynamic physiological conditions such as caffeine intake.

What is Already Known: Existing methods like CPDA and EBA are used in clinical settings, but their sensitivity to noise and subtle hemodynamic changes varies significantly.

What this Paper Adds: This study compares three signal processing techniques—CPDA, EBA, and WTA—demonstrating that wavelet-based analysis (WTA) offers superior noise resistance and sensitivity to caffeine-induced changes in stroke volume and cardiac output.

Who would benefit: Researchers and developers of wearable health technologies, clinicians involved in remote cardiovascular monitoring, and biomedical engineers working on personalized diagnostics.

References

1. Sherwood(Chair) A, Allen MT, Fahrenberg J, Kelsey RM, Lovallo WR, Doornen LJP. Methodological Guidelines for Impedance Cardiography. Psychophysiology. 1990;27(1):1-23. doi:10.1111/j.1469-8986.1990.tb02171.x
2. Cybulski G. Ambulatory Impedance Cardiography. Vol 76. Springer Berlin Heidelberg; 2011. doi:10.1007/978-3-642-11987-3
3. Schmidt C, Theilmeier G, Aken HV, et al. Comparison of electrical velocimetry and transoesophageal Doppler echocardiography for measuring stroke volume and cardiac output † †Declaration of interest. This study was supported by Osypka Medical GmbH, Berlin, Germany. Br J Anaesth. 2005;95(5):603-610. doi:10.1093/bja/aei224
4. Klabunde R. Cardiovascular Physiology Concepts. Lippincott Williams & Wilkins; 2011.
5. Lewis RP, Rittogers SE, Froester WF, Boudoulas H. A critical review of the systolic time intervals. Circulation. 1977;56(2):146-158. doi:10.1161/01.cir.56.2.146
6. Karpiel I, Richter-Laskowska M, Feige D, Gacek A, Sobotnicki A. An Effective Method of Detecting Characteristic Points of Impedance Cardiogram Verified in the Clinical Pilot Study. Sensors. 2022;22(24):24. doi:10.3390/s22249872
7. Talley RC, Meyer JF, McNay JL. Evaluation of the pre-ejection period as an estimate of myocardial contractility in dogs. Am J Cardiol. 1971;27(4):384-391. doi:10.1016/0002-9149(71)90435-8

8. Mozaffarian D, Benjamin EJ, Go AS, et al. Heart Disease and Stroke Statistics—2015 Update: A Report From the American Heart Association. Circulation. 2015;131(4). doi:10.1161/cir.0000000000000152
9. Pare G, Jaana M, Sicotte C. Systematic Review of Home Telemonitoring for Chronic Diseases: The Evidence Base. J Am Med Inform Assoc. 2007;14(3):269-277. doi:10.1197/jamia.m2270
10. Bui AL, Fonarow GC. Home Monitoring for Heart Failure Management. J Am Coll Cardiol. 2012;59(2):97-104. doi:10.1016/j.jacc.2011.09.044
11. Etemadi M, Inan OT, Giovangrandi L, Kovacs GTA. Rapid Assessment of Cardiac Contractility on a Home Bathroom Scale. IEEE Trans Inf Technol Biomed. 2011;15(6):864-869. doi:10.1109/titb.2011.2161998
12. Inan OT, Migeotte PF, Park KS, et al. Ballistocardiography and Seismocardiography: A Review of Recent Advances. IEEE J Biomed Health Inform. 2015;19(4):1414-1427. doi:10.1109/jbhi.2014.2361732
13. Inan OT, Etemadi M, Wiard RM, Giovangrandi L, Kovacs GTA. Robust ballistocardiogram acquisition for home monitoring. Physiol Meas. 2009;30(2):169-185. doi:10.1088/0967-3334/30/2/005
14. Javaid AQ, Wiens AD, Fesmire NF, Weitnauer MA, Inan OT. Quantifying and Reducing Posture-Dependent Distortion in Ballistocardiogram Measurements. IEEE J Biomed Health Inform. 2015;19(5):1549-1556. doi:10.1109/jbhi.2015.2441876
15. Adamson PB, Magalski A, Braunschweig F, et al. Ongoing right ventricular hemodynamics in heart failure. J Am Coll Cardiol. 2003;41(4):565-571. doi:10.1016/s0735-1097(02)02896-6
16. Heidenreich PA, Trogdon JG, Khavjou OA, et al. Forecasting the Future of Cardiovascular Disease in the United States: A Policy Statement From the American Heart Association. Circulation. 2011;123(8):933-944. doi:10.1161/cir.0b013e31820a55f5
17. Pelczyńska M, Bogdański P. Prozdrowotne właściwości kawy (eng. "The health benefits of coffee"). Medica. 2019;3(4):311-317.
18. Niroshana SMI, Kuroda S, Tanaka K, Chen W. Beat-wise segmentation of electrocardiogram using adaptive windowing and deep neural network. Sci Rep. 2023;13(1):11039. doi:10.1038/s41598-023-37773-y
19. Xie C. Biomedical Signal Processing: An ECG Application. In: Celi LA, Majumder MS, Ordóñez P, Osorio JS, Paik KE, Somai M, eds. Leveraging Data Science for Global Health. Springer International Publishing; 2020:285-303. doi:10.1007/978-3-030-47994-7_17
20. Forouzanfar M, Baker FC, Colrain IM, Goldstone A, Zambotti M. Automatic analysis of pre-ejection period during sleep using impedance cardiogram. Psychophysiology. 2019;56(7):e13355. doi:10.1111/psyp.13355
21. Pan J, Tompkins WJ. A Real-Time QRS Detection Algorithm. IEEE Trans Biomed Eng. 1985;BME-32(3):230-236. doi:10.1109/TBME.1985.325532
22. Forouzanfar M, Baker FC, de Zambotti M, McCall C, Giovangrandi L, Kovacs GTA. Toward a better noninvasive assessment of preejection period: A novel automatic algorithm for B-point detection and correction on thoracic impedance cardiogram. Psychophysiology. 2018;55(8):e13072. doi:10.1111/psyp.13072
23. Dehkordi P, Khosrow-Khavar F, Di Rienzo M, et al. Comparison of Different Methods for Estimating Cardiac Timings: A Comprehensive Multimodal Echocardiography Investigation. Front Physiol. 2019;10:1057. doi:10.3389/fphys.2019.01057
24. Trybek P, Sobotnicka E, Wawrzkiewicz-Jałowiecka A, et al. A New Method of Identifying Characteristic Points in the Impedance Cardiography Signal Based on Empirical Mode Decomposition. Sensors. 2023;23(2):675. doi:10.3390/s23020675
25. Darling CE, Dovancescu S, Saczynski JS, et al. Bioimpedance-Based Heart Failure Deterioration Prediction Using a Prototype Fluid Accumulation Vest-Mobile Phone Dyad: An Observational Study. JMIR Cardio. 2017;1(1):e6057. doi:10.2196/cardio.6057
26. Mansouri S, Alhadidi T, Chabchoub S, Salah RB. Impedance cardiography: recent applications and developments. Biomed Res. 2018;29(19). doi:10.4066/biomedicalresearch.29-17-3479
27. Chabchoub S, Mansouri S, Salah RB. Impedance cardiography signal denoising using discrete wavelet transform. Australas Phys Eng Sci Med. 2016;39(3):655-663. doi:10.1007/s13246-016-0460-z
28. Lipinski P, Yatsymirskyy M. Efficient 1D and 2D Daubechies Wavelet Transforms with Application to Signal Processing. In: Beliczynski B, Dzielinski A, Iwanowski M, Ribeiro B, eds. Adaptive and Natural Computing Algorithms. Springer; 2007:391-398. doi:10.1007/978-3-540-71629-7_44
29. Escalona O, Cullen N, Weli I, McCallan N, Ng KY, Finlay D. Robust Arm Impedocardiography Signal Quality Enhancement Using Recursive Signal Averaging and Multi-Stage Wavelet Denoising Methods for Long-Term Cardiac Contractility Monitoring Armbands. Sensors. 2023;23(13):5892. doi:10.3390/s23135892
30. Hall JE, Hall ME. Guyton and Hall Textbook of Medical Physiology. 14th edition. Elsevier; 2021.
31. De Simone G, Devereux RB, Daniels SR, et al. Stroke Volume and Cardiac Output in Normotensive Children and Adults: Assessment of Relations With Body Size and Impact of Overweight. Circulation. 1997;95(7):1837-1843. doi:10.1161/01.cir.95.7.1837
32. Collis T, Devereux RB, Roman MJ, et al. Relations of Stroke Volume and Cardiac Output to Body Composition: The Strong Heart Study. Circulation. 2001;103(6):820-825. doi:10.1161/01.CIR.103.6.820
33. Lavie CJ, Milani RV, Ventura HO. Obesity and Cardiovascular Disease. J Am Coll Cardiol. 2009;53(21):1925-1932. doi:10.1016/j.jacc.2008.12.068
34. Mesas AE, Leon-Muñoz LM, Rodriguez-Artalejo F, Lopez-Garcia E. The effect of coffee on blood pressure and cardiovascular disease in hypertensive individuals: a systematic review and meta-analysis. Am J Clin Nutr. 2011;94(4):1113-1126. doi:10.3945/ajcn.111.016667
35. Stepanov R, Podtaev S, Dumler A, Chugainov S. Assessment of cardiac time intervals by wavelet transform of the impedance cardiogram. Technol Health Care. 2016;24(s2):S803-S809. doi:10.3233/THC-161213
36. Stepanov R, Dumler A, Podtaev S, Frick P. Wavelet Analysis in Impedance Rheocardiography. In: Simini F, Bertemes-Filho P, eds. Bioimpedance in Biomedical Applications and Research. Springer International Publishing; 2018:257-269. doi:10.1007/978-3-319-74388-2_13
37. Guo T, Zhang T, Lim E, Lopez-Benitez M, Ma F, Yu L. A Review of Wavelet Analysis and Its Applications: Challenges and Opportunities. IEEE Access. 2022;10:58869-58903. doi:10.1109/access.2022.3179517
38. Evans JM, Wang S, Greb C, et al. Body Size Predicts Cardiac and Vascular Resistance Effects on Men's and Women's Blood Pressure. Front Physiol. 2017;8. doi:10.3389/fphys.2017.00561
39. Pale U, Müller N, Arza A, Atienza D. ReBeatICG: Real-time Low-Complexity Beat-to-beat Impedance Cardiogram Delineation Algorithm. In: 2021 43rd Annual International Conference of the IEEE Engineering in Medicine & Biology Society (EMBC). 2021:5618-5624. doi:10.1109/EMBC46164.2021.9630170
40. Lozano DL, Norman G, Knox D, et al. Where to B in dZ/dt. Psychophysiology. 2007;44(1):113-119. doi:10.1111/j.1469-8986.2006.00468.x
41. Árbol J, Perakakis P, Garrido A, Mata J, Fernández-Santaella M, Vila J. Mathematical detection of aortic valve opening (B point) in impedance cardiography: A comparison of three popular algorithms. Psychophysiology. 2017;54:350-357. doi:10.1111/psyp.12799

42. Sheikh SA, Gurel NZ, Gupta S, et al. Data-driven approach for automatic detection of aortic valve opening: B point detection from impedance cardiogram. Psychophysiology. 2022;59(12):e14128. doi:10.1111/psyp.14128

43. Almeida BA, Morales AP, Ribeiro JRC, et al. Impact of Caffeine Intake Strategies on Heart Rate Variability duringPost-Exercise Recovery: A Systematic Review and Meta-Analysis. Curr Cardiol Rev. 2024;20(3). doi:10.2174/011573403x289842240307114736

44. Benjamim CJR, Monteiro LRL, Pontes YMDM, et al. Caffeine slows heart rate autonomic recovery following strength exercise in healthy subjects. Rev Port Cardiol. 2021;40(6):399-406. doi:10.1016/j.repc.2020.07.015

45. Alsene K, Deckert J, Sand P, De Wit H. Association Between A2a Receptor Gene Polymorphisms and Caffeine-Induced Anxiety. Neuropsychopharmacology. 2003;28(9):1694-1702. doi:10.1038/sj.npp.1300232

46. Nehlig A. Effects of coffee/caffeine on brain health and disease: What should I tell my patients? Pract Neurol. 2016;16(2):89-95. doi:10.1136/practneurol-2015-001162